Journal of the Korean Nuclear Society
Volume 31, Number 3, pp.303~313, June 1999

Comparison of Interpolation Methods for Reconstructing Pin-wise Power Distribution in Hexagonal Geometry

Hyung-Seok Lee and Won Sik Yang
Chosun University
375 Su Seosuk-dong, Dong-gu, Kwangiu, 501-759, Korea
wsyang@chosun.ac.kr

(Received December 1, 1998)

Abstract

Various interpolation methods have been compared for reconstruction of LMR pin power distributions in hexagonal geometry. Interpolation functions are derived for several combinations of nodal quantities and various sets of basis functions, and tested against fine mesh calculations. The test results indicate that the interpolation functions based on the sixth degree polynomial are quite accurate, yielding maximum interpolation errors in power densities less than 0.5%, and maximum reconstruction errors less than 2% for driver assemblies and less than 4% for blanket assemblies. The main contribution to the total reconstruction error is made by the nodal solution errors and the corner point flux errors. For the polynomial interpolations, the basis monomial set needs to be selected such that the highest powers of x and y are as close as possible. It is also found that polynomials higher than the seventh degree are not adequate because of the oscillatory behavior.

Key Words : hexagonal geometry, pin power reconstruction, polynomial interpolation

1. Introduction

Advanced nodal methods have become standard tools for core design and analysis by replacing the conventional fine-mesh finite difference methods. This is due to the high accuracy and efficiency of the coarse-mesh nodal schemes and the capabilities to recover pin-wise information from coarse mesh solutions. The reconstruction methods to extract the pin-wise power distributions from coarse reactor representations have been studied extensively and have reached a high level of development for light water reactors (LWRs) in Cartesian geometry.[1-7] All these methods intuitively assume that the detailed flux shape in an assembly can be approximated by a superposition of a detailed inner assembly form function on a smoother intra-nodal shape function. The assembly form factor is derived from the single assembly calculations. The intra-nodal flux shapes are derived from the nodal solution consisting of nodal fluxes and surface currents. The methods developed for the reconstruction of homogeneous intra-nodal fluxes include

polynomial[1-2] and exponential interpolation methods[3-4], analytical methods[5], and direct solver methods based on finite difference techniques[6].

Relatively a few studies have been performed for hexagonal geometry. A reconstruction method for hexagonal geometry was first proposed by Yang et al.[8] for predicting pin burnup characteristics of liquid metal reactors (LMRs). In this method, the intra-nodal flux distributions are interpolated using sixth order polynomials constrained to satisfy the nodal information. More recently, Finnemann et al.[9] and Yamaoka et al.[10] proposed direct solver methods. In these methods, the boundary conditions for each assembly are first interpolated using the global solution, and then the diffusion equations for each assembly are solved with the constructed boundary conditions. In the former method, the global solution is obtained with a nodal method, and the diffusion equations are solved with a finite difference method. On the other hand, in the latter method, the global solution is obtained with a finite difference method, and the diffusion equations are solved with a Green's function method.

In this paper, we investigate the interpolation methods for reconstructing pin power distributions in hexagonal geometry in more detail by extending the study in reference 8, since they are more efficient than the direct solver methods. Specifically, we have examined various ways for reconstructing intra-nodal flux distributions from full core nodal diffusion calculations performed in hexagonal geometry using the nodal option[11] of the DIF3D code[12]. As alternatives to the interpolating polynomial employed in reference 8, various combinations of nodal quantities and different basis functions are investigated. In addition to the collocation method used in reference 8, the least square method is employed to determine the expansion coefficients. Section 2 describes these variations of interpolation methods. Section 3 presents the results of numerical tests for a liquid metal reactor, and Section 4 concludes the paper.

2. Reconstruction Methods

The DIF3D nodal scheme employs a nodal expansion method and the interface current formulation for solving the multi-group diffusion equation. In hexagonal-z geometry problems, the nodal unknowns for each node and each energy group are five flux moments and eight interface partial currents. Equivalently, the nodal information for each node and each group consists of one node-averaged flux, eight surface-averaged fluxes, eight surface-averaged net currents, and four flux moments (one for each axis of the hexagonal prism).

In the interpolation methods, each intra-nodal flux distribution is approximated by a function in a predetermined function space such that the resulting function reproduces a desired set of the above nodal values. For example, in reference 8, the flux within a node is assumed to be separable in the hexagonal plane and axial directions, and then the axial and hexagonal plane flux distributions are interpolated with a cubic polynomial and a sixth order polynomial of two variables, respectively. The interpolation coefficients are determined by requiring these polynomials to reproduce desired subsets of nodal quantities and local corner point fluxes. The corner fluxes are approximated using the nodal quantities of the three nodes surrounding a corner point and additional continuity conditions.

In this study, we employ the same separability assumption used in reference 8 and focus on the reconstruction of the hexagonal plane flux distributions. Various combinations of constraints and different basis functions are investigated. In

Table 1. Linear Functionals Associated with Nodal Quantities

Nodal Quantity	Linear Functional
Node-averaged flux	$L_{av}(\phi)=\frac{1}{V}\int_V \phi(x,y)dxdy$ V = node volume
Surface-averaged flux	$L_i^s(\phi)=\frac{1}{A}\int_{S_i}\phi[x(s),y(s)]ds \quad (i=1,2,\cdots,6)$ A = surface area
Surface-averaged net current	$L_i^J(\phi)=-\frac{D}{A}\int_{S_i}\boldsymbol{n}_i\cdot\nabla\phi[x(s),y(s)]ds \quad (i=1,2,\cdots,6)$ D = diffusion coefficient $\boldsymbol{n}_i$ = unit normal vector of surface S_i
Planar moment	$L_i^M(\phi)=\frac{1}{V}\int_V w_i(x,y)\phi(x,y)dxdy \quad (i=x,u,v)$ $w_x(x,y)=sgn(x)$ $w_u(x,y)=sgn(y+x/\sqrt{3})$ $w_v(x,y)=sgn(y-x/\sqrt{3})$
Corner point flux	$L_i^c(\phi)=\phi(x_i,y_i) \quad (i=1,2,\cdots,6)$ $x_i=l\cos\frac{(2i-1)\pi}{6}$, $y_i=l\sin\frac{(2i-1)\pi}{6}$ l = side length
Flux derivative at corner point	$L_i^{d+}(\phi)=\boldsymbol{t}_{i+1}\cdot\nabla\phi(x_i,y_i)$ $L_i^{d-}(\phi)=\boldsymbol{t}_i\cdot\nabla\phi(x_i,y_i)$ $\boldsymbol{t}_i$ = unit tangent vector of surface S_i

addition to the above nodal quantities, the fluxes and flux derivatives at corner points are included in the constraints. Using a method similar to that of reference 8, the flux and flux derivatives at a corner point are determined in terms of the nodal quantities and diffusion coefficients of the three nodes surrounding a corner point.

To determine the flux and flux derivatives at a corner point, the planar flux distribution is assumed to be biquadratic (less the x^2 y^2 term) in each of the three nodes surrounding a corner point. A system of 24 equations (for the eight coefficients of this expansion in each of the three nodes) can be obtained by (a) requiring the node-averaged fluxes, surface-averaged fluxes, and surface-averaged net currents to be reproduced, (b) enforcing additional continuity conditions on the midpoint net currents and on the flux derivatives at a corner point in the tangential directions of interfaces, and (c) imposing a source-free condition at a corner point. By solving these equations for the coefficients, the planar flux distribution in each node is obtained. The flux and flux derivatives at a corner point are determined by evaluating the resulting planar flux distribution.

2.1. Polynomial Interpolation Methods

If the hexagonal plane flux distribution is interpolated for each group g by a polynomial in an N-dimensional polynomial space F_N, then it can be represented as

$$\phi_g(x,y) = \sum_{n=1}^{N} c_n^g f_n(x,y) \quad (1)$$

where $\{f_1, f_2, \cdots, f_N\}$ is the basis of F_N. The expansion coefficients c_n^g are determined by the collocation method in which a desired set of nodal quantities and corner point values are required to be reproduced exactly by the resulting polynomial. Each of the nodal quantities and corner point values can be associated with a linear functional defined on the function space F_N as shown in Table 1. Therefore, if $\{L_1, L_2, \cdots, L_M\}$ is the set of the linear functionals associated with the nodal quantities required to be reproduced, this leads to the problem of finding the coefficient vector $\boldsymbol{c}$ for a given vector of nodal values $\boldsymbol{\omega} = (\omega_1, \omega_2, \cdots, \omega_M)^T$ such that

$$\boldsymbol{Lc} = \boldsymbol{\omega} \quad (2)$$

where $\boldsymbol{L}$ is the generalized Gram matrix whose element in the m-th row and the n-th column is $L_m(f_n)$.

This problem can be solved only if L_m's are independent in the algebraic conjugate space of F_N, say F_N^*.[13] That is, the rank of the $M \times N$ matrix $\boldsymbol{L}$ must be M. In order for the rank of $\boldsymbol{L}$ to be M, it is necessary to choose the function space such that $N \geq M$. However, this is not a sufficient condition. The M linear functionals are not always independent in F_N^* even when $N > M$. Therefore, the minimum degree of the polynomial and the associated sets of basis functions with which the given nodal information can be reproduced were first determined by evaluating the generalized Gram matrix analytically and by reducing it to the row-echelon form. Table 2 shows the minimum degree of polynomial for several combinations of the available nodal quantities and the fluxes and flux derivatives at six corner points.

As shown in Table 2, the dimension of the minimal polynomial space is generally greater than the number of constraints. As a result, the interpolation polynomial cannot be determined uniquely with the given constraints. In order to determine the unique interpolation polynomial in each minimal polynomial space, the subspaces whose dimension is equal to the number of constraints and in which the associated linear functionals are independent were determined by examining independent monomials. Using these subspaces, several numerical tests were performed to evaluate the accuracy of interpolation schemes. Reference solutions were calculated using the triangular finite difference option of DIF3D with very fine triangular meshes. For the purpose of these preliminary tests, the values of nodal and corner point quantities were obtained by utilizing the reference solutions. Using these nodal and corner values, the hexagonal plane flux distributions were interpolated in each of these subspaces and compared to the finite difference reference solution.

These numerical tests showed that the interpolation accuracy strongly depends on the selected set of basis functions. Among the various subsets of the independent monomials with respect to the given set of linear functionals, the best interpolation accuracy was given by the subset selected such that the highest powers of x and y are as close as possible. Based on these test results, the monomials in this subset were selected as basis functions. These basis monomials are included in Table 2 for several combinations of nodal quantities and corner values.

Since the generalized Gram matrix can be evaluated analytically,[8] Eq. (2) can be solved analytically for arbitrary values of nodal quantities. As a result, the coefficients of basis monomials in Eq. (1) are obtained as linear combinations of selected nodal quantities, and the interpolation polynomial is uniquely determined. This

Table 2. Minimum Degree of Polynomial and Basis Monomials for Various Combination of Nodal Quantities

Case	Nodal Quantities[a]	Number of Constraints	Minimum Degree of Polynomial	Basis Monomials
Ⅰ	NAV SAVs SNDs CPVs	19	6 (28)[b]	1, x, y, x^2, xy, y^2, x^3, x^2y, xy^2, y^3, x^4, x^3y, x^2y^2, xy^3, y^4, x^3y^2, x^2y^3, xy^4, x^2y^4
Ⅱ	NAV SAVs SNDs CPVs PMTs	22	7 (36)	1, x, y, x^2, xy, y^2, x^3, x^2y, xy^2, y^3, x^4, x^3y, x^2y^2, xy^3, y^4, x^5, x^4y, x^3y^2, x^2y^3, xy^4, x^2y^4, x^3y^4
Ⅲ	NAV SAVs SNDs CPVs CPDs	31	8 (45)	1, x, y, x^2, xy, y^2, x^3, x^2y, xy^2, y^3, x^4, x^3y, x^2y^2, xy^3, y^4, x^5, x^4y, x^3y^2, x^2y^3, xy^4, y^5, x^6, x^5y, x^4y^2, x^3y^3, x^2y^4, xy^5, x^5y^2, x^4y^3, x^3y^4, x^4y^4
Ⅳ	NAV SAVs SNDs CPVs CPDs PMTs	34	9 (55)	1, x, y, x^2, xy, y^2, x^3, x^2y, xy^2, y^3, x^4, x^3y, x^2y^2, xy^3, y^4, x^5, x^4y, x^3y^2, x^2y^3, xy^4, y^5, x^6, x^5y, x^4y^2, x^3y^3, x^2y^4, xy^5, x^5y^2, x^4y^3, x^3y^4, x^2y^5, xy^6, x^4y^4, x^5y^4

[a]NAV = node-averaged flux, SAV = surface-averaged flux,
SND = surface-averaged normal derivative, PMT = planar moment,
CPV = corner point flux, CPD = corner point flux derivative
[b]Dimension of the corresponding polynomial space

interpolation function can be further manipulated to be invariant under the symmetry transformations of hexagon[14] by performing 12 symmetry transformations of hexagon on this interpolation polynomial with appropriate permutations of nodal and corner values and by taking an average of the 12 resulting functions. For example, for a given set of node-averaged flux $\overline{\phi}_g$, surface-averaged fluxes ϕ^s_{gi}, corner point fluxes ϕ^c_{gi}, surface-averaged net currents J^s_{gi}, flux derivatives at corner points $d^{c\pm}_{gi}$, and planar flux moments ϕ^m_{gi}, the hexagonal plane distribution of the g-th group flux is determined as

$$\begin{aligned}\phi_g(x,y) = {} & \overline{\phi}_g F^{av}(x,y) + \sum_{i=1}^{6}\{\phi^s_{gi} F^s_i(x,y) + \phi^c_{gi} F^c_i(x,y) \\ & + J^s_{gi} F^J_i(x,y) + d^{c+}_{gi} F^{d+}_i(x,y) + d^{c-}_{gi} F^{d-}_i(x,y)\} \\ & + \sum_{i=1}^{3}\phi^m_{gi} F^m_i(x,y)\end{aligned} \quad (3)$$

where F s are the cardinal functions[15] corresponding to individual nodal quantities. The functional forms of cardinal functions depend on

the selected nodal quantities and basis monomials. However, in each interpolation method, they form a biorthonormal set for the linear functionals corresponding to the nodal quantities to be reproduced.

2.2. Least Square Method

The nodal values calculated with the nodal expansion method are not exact, but have some errors. Especially, the planar flux moments have relatively large errors compared to the values determined using the fine-mesh finite difference solution. Furthermore, the fluxes and flux derivatives at a corner point are determined approximately using the nodal values and diffusion coefficients of the three nodes surrounding a corner point. Therefore, it may not be the best way to determine the expansion coefficients in Eq. (1) such that the reconstructed flux distribution reproduces the nodal quantities exactly.

As an alternative to the collocation method, the least square method has been tried. In this method, the expansion coefficients in Eq. (1) are determined such that the 2-norm of the difference in nodal information between the reconstructed flux distribution and the nodal calculation is minimized. Specifically, it has been tried to improve the expansion coefficients of the collocation method by reflecting the additional nodal information which are not used in determining the coefficients. Using the cardinal functions of the case I of the polynomial interpolation methods (where one node-averaged flux $\overline{\phi}_g$, six surface-averaged fluxes ϕ^s_{gi}, six surface-averaged net currents J^s_{gi}, and six corner point fluxes ϕ^c_{gi} are used), the hexagonal plane flux distribution was expanded as

$$\phi_g(x,y) = \sum_{i=1}^{19} a_{gi} F_i(x,y) \tag{4}$$

In the collocation method, the coefficient a_{gi} of each cardinal function is given by the corresponding nodal or corner value as discussed in the previous subsection. In the least square method, these coefficients are re-estimated by utilizing additional three planar moments (note that corner values are not given by nodal calculations).

Applying the 22 linear functionals corresponding to the 22 nodal or corner quantities to Eq. (4) in an appropriate order, we obtain the following matrix equation in which the number of equations are more than unknowns:

$$\begin{pmatrix} \boldsymbol{I} \\ \boldsymbol{B} \end{pmatrix} \boldsymbol{a} = \begin{pmatrix} \boldsymbol{\phi}_1 \\ \boldsymbol{\phi}_2 \end{pmatrix} \tag{5}$$

where $\boldsymbol{I}$ is the 19×19 identity matrix and $\mathbf{B}$ is the 3×19 matrix composed of the images of cardinal functions F_i with respect to the three functionals corresponding to the planar moments. The vector $\boldsymbol{a}$ is the unknown coefficient vector, $\boldsymbol{\phi}_1$ is the vector composed of the above 19 nodal or corner quantities, and $\boldsymbol{\phi}_2$ is the vector composed of three planar moments.

Denoting the matrix on the left-hand side and the vector on the right-hand side of Eq. (5) by $\boldsymbol{A}$ and $\boldsymbol{\phi}$, respectively, the least square solution of Eq. (5) is given by the vector $\boldsymbol{a}$ that minimizes $\| \mathbf{Aa} - \boldsymbol{\phi} \|_2$. Consequently, the coefficient vector $\boldsymbol{a}$ is given by the solution of the following matrix equation:

$$(\boldsymbol{I} + \boldsymbol{B}^T \boldsymbol{B}) \boldsymbol{a} = \boldsymbol{\phi}_1 + \boldsymbol{B}^T \boldsymbol{\phi}_2 \tag{6}$$

where bold $\boldsymbol{B}^T$ is the transpose of $\boldsymbol{B}$. By solving this equation, the expansion coefficients are obtained as the linear combinations of 22 nodal or local quantities. Here, it is noteworthy that the coefficient of cardinal function F_{av} becomes just the node-averaged flux as in the case of the collocation method. This is due to fact that the

images of the cardinal function F_{av} with respect to the functionals associated with three planar moments are zero. In other words, the node-averaged flux, which is more accurate than the other nodal quantities, is reproduced by this least square method.

2.3. Hybrid Function Interpolation Method

The multi-group diffusion equation for a homogenized hexagonal node can be represented as

$$-\nabla^2\phi_g(x,y) + \varkappa_g^2\phi_g(x,y) = S_g(x,y) \qquad (7)$$

where $\varkappa_g^2 = \Sigma_{rg}/D_g$ and S_g is the fission and scattering source in group g. Σ_{rg} and D_g are the removal cross section and the diffusion coefficient, respectively. Even though S_g and ϕ_g are not independent because of the fission source, an approximate solution of Eq. (7) can be obtained by assuming that they are independent. In this case, the solution is given by a sum of the homogeneous solution of Helmholtz equation and the particular solution due to the source S_g.

If we approximate the source S_g by projecting it on a polynomial space, the particular solution of Eq. (7) can be approximated by a polynomial. In addition, the solution of Helmholtz equation can be represented as an infinite sum of the exponential functions $e^{\pm\varkappa_g(\xi_m x + \eta_m y)}$ over all unit vectors (ξ_m, ξ_m). If this summation is truncated, the solution of Eq. (7) can be approximated by a linear combination of exponential functions and a polynomial. Based on this observation, it has been tried to interpolate the hexagonal plane distribution using the basis functions composed of a polynomial and exponential functions.

In this method, the fourth order polynomial and the exponential functions in the directions normal to each surface of the hexagon was used as basis functions. That is, the hexagonal plane flux distribution was expanded as

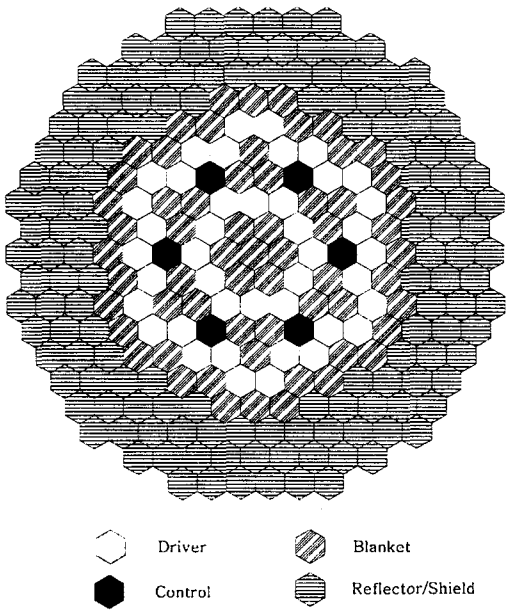

Fig. 1. Planar Layout of 450 MWt LMR Core.

$$\begin{aligned}\phi_g(x,y) = {} & a_1 + a_2x + a_3y + a_4x^2 + a_5xy + a_6y^2 + a_7x^3 + a_8x^2y \\ & + a_9xy^2 + a_{10}y^3 + a_{11}x^4 + a_{12}xy^3 + a_{13}y^4 \\ & + b_1e^{\varkappa_g x} + b_2e^{\varkappa_g(x+\sqrt{3}y)/2} + b_3e^{-\varkappa_g(x-\sqrt{3}y)/2} \\ & + b_4e^{-\varkappa_g x} + b_5e^{-\varkappa_g(x+\sqrt{3}y)/2} + b_6e^{\varkappa_g(x-\sqrt{3}y)/2}\end{aligned} \qquad (8)$$

The 19 expansion coefficients were determined by the collocation method such that one node-averaged flux, six surface-averaged fluxes, six corner point fluxes, and six surface-averaged net currents are reproduced.

3. Numerical Tests

The accuracy of the above reconstruction methods has been tested by performing

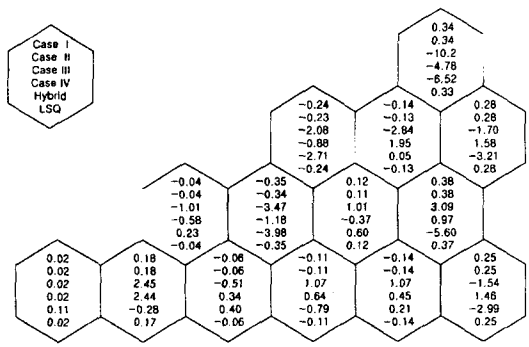

Fig. 2. Maximum Interpolation Errors (%) in Power Densities.

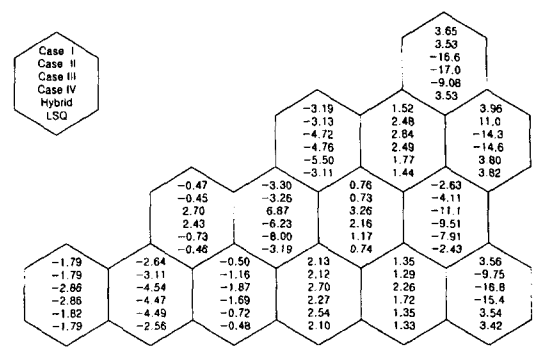

Fig. 3. Maximum Reconstruction Errors (%) in Power Densities.

benchmark calculations for a two-dimensional (mid-plane) representation of a 450 MWt liquid metal reactor[16]. As shown in Figure 1, this core is a small heterogeneous core with internal blankets, and hence the leakage effect is relatively large. Reflector and shield assemblies surround the whole core, and the hexagonal lattice pitch is 16 cm. The reference solution was obtained by performing a nine-group diffusion calculation with the one-sixth-core model. The triangular finite difference option of the DIF3D was used in this calculation with 864 triangular meshes per each hexagon.

The group fluxes and power density in each triangular mesh were reconstructed using the reconstruction methods described in the previous section, and compared to the reference solution. In order to determine the error contributions attributable to the errors in the nodal information provided by the DIF3D nodal scheme and the approximations in the reconstruction schemes, separate interpolation calculations were also performed using the nodal and corner values collapsed from the reference solution. These calculations give the interpolation errors due to the approximations in each interpolation method.

Figure 2 shows the maximum interpolation errors in power densities for individual driver and blanket assemblies. These results show that the interpolation functions (of the case I, II of the polynomial interpolation methods, and the least square method) based on the sixth or seventh degree polynomial are excellent. Even in the blanket assemblies which have large flux gradients and small power densities, the maximum errors are less than 0.4%. Except one assembly, all these maximum errors occurred at the assembly periphery. However, the eighth degree polynomial of the case III and the ninth degree polynomial of the case IV result in large interpolation errors. In general, these large errors occurred around the middle part between the center of hexagon and surfaces. This is due to the oscillatory behavior of higher order polynomials[15] and the nodal information concentrated on the node interfaces. The hybrid interpolation method also shows large interpolation errors in blanket assemblies. This implies that a fourth order polynomial and the exponential functions in the directions normal to the surfaces are not adequate to represent large flux gradients accurately.

It is worth mentioning again that the interpolation accuracy strongly depends on the selected set of basis functions even when the same

set of nodal information and the same polynomial space are used in the interpolation. For example, from the preliminary numerical tests discussed in Section 2.1, it was found that the sixth degree polynomial of the case I of the polynomial interpolation methods is more accurate up to about five times than other sixth order polynomials derived with the same nodal information but different basis monomials. For a given set of nodal information, among the various sets of the independent monomials with respect to the associated functionals, it is desirable to select the monomial set such that the highest powers of x and y are as close as possible.

Figure 3 shows the maximum reconstruction errors (including the errors in the nodal information) in power densities for individual driver and blanket assemblies. These results show that the sixth degree polynomials of the case I of the polynomial interpolation methods and the least square method are better than the other interpolation functions. The maximum errors in the reconstructed power densities are less than 2% for driver assemblies and less than 4% for blanket assemblies. The least square method is only slightly better than the case I of the polynomial interpolation methods. This result and the interpolation errors shown in Figure 2 indicate that the planar moments do not improve the interpolation accuracy much.

Comparing these reconstruction errors to the interpolation errors, it can be seen that the nodal solution errors and the corner point flux errors make much larger contribution to the reconstruction error than the interpolation error itself. In order to determine the errors due to the corner flux approximation separately, interpolation calculations were also performed using the reference nodal values and the approximate corner fluxes, which were computed with the reference nodal values as described in Section 2. The maximum errors in the reconstructed power densities are less than 1, 2, and 3% for driver, internal blanket, and radial blanket assemblies, respectively. By comparing these power densities with those reconstructed with the nodal solution, the reconstruction errors attributable to the nodal information were found to be less than 1.5, 2.5, and 4% for driver, internal blanket, and radial blanket assemblies, respectively. These results indicate that the maximum errors due to the nodal information and the corner flux approximation are not additive since they occur at different positions. The maximum errors due to the corner flux approximation always occurred at corner points, while the maximum errors due to the nodal information generally occurred around the midpoints of interfaces.

Compared to the interpolation errors, the reconstruction errors of the seventh degree polynomial of the case II of the polynomial interpolation methods are very large in radial blanket assemblies adjacent to reflectors. (Note that the interpolation accuracy of this case is slightly better than the case I.) This implies that the planar moments of these assemblies calculated with the DIF3D nodal scheme have relatively large errors. In fact, these assemblies have large flux gradients, and hence relatively large planar moments. As a result, the absolute errors in planar moments calculated with the nodal scheme are also relatively larger for these assemblies.

4. Conclusions

Various interpolation methods have been examined for reconstruction of LMR pin power distributions from nodal diffusion calculations performed in hexagonal geometry using the nodal option of the DIF3D code. For several combinations of nodal quantities, interpolation

functions are derived using various sets of basis functions. The collocation method and the least square method are employed to determine the expansion coefficients. The accuracy of these interpolation functions has been tested by performing benchmark calculations for a 450 MWt LMR.

The test results indicate that the interpolation functions based on the sixth and seventh degree polynomials are quite accurate, yielding maximum interpolation errors in power densities less than 0.4%. The sixth degree polynomials obtained by the collocation and the least square method yield maximum reconstruction errors that are less than 2% for driver assemblies and less than 4% for blanket assemblies. The main contribution to the reconstruction error is made by the nodal solution errors and the corner point flux errors. In order to improve the overall accuracy, therefore, it is necessary to reduce the nodal solution error.

The interpolation accuracy strongly depends on the selected set of basis functions even when the same set of nodal information and the same polynomial space are used in the interpolation. As a result, it is desirable to select the basis monomial set such that the highest powers of x and y are as close as possible. It is also found that polynomials lower than the fifth degree cannot represent the large flux gradients in small heterogeneous core accurately. Polynomials higher than the seventh degree are not adequate either because of the oscillatory behavior.

References

1. K. Koebke and M. R. Wagner, "The Determination of the Pin Power Distribution in a Reactor Core on the Basis of Nodal Coarse Mesh Calculations," *Atomkernenergie*, **30**, 136 (1977).
2. H. S. Khalil, P. J. Finck, and A. F. Henry, "Reconstruction of Fuel Pin Powers from Nodal Results," *Proc. Topl. Mtg. Advances in Reactor Computations*, Salt Lake City, Utah, March 28-31, 1983, Vol. I, p. 367, American Nuclear Society (1983).
3. K. Koebke and L. Hetzelt, "On the Reconstruction of Local Homogeneous Neutron Flux and Current Distributions of Light Water Reactors from Nodal Schemes," *Nucl. Sci. Eng.*, **91**, 123 (1985).
4. K. R. Rempe, K. S. Smith, and A. F. Henry, "SIMULATE-3 Pin Power Reconstruction: Methodology and Benchmarking," *Proc. Int. Reactor Physics Conf.*, Jackson Hole, Wyoming, September 18-22, 1988, Vol. III, p. 19, American Nuclear Society (1988).
5. R. Böer and H. Finnemann, "Fast Analytical Flux Reconstruction Method for Nodal Space-Time Nuclear Reactor Analysis," *Ann. Nucl. Energy*, **19**, 617-628 (1992).
6. H. Finnemann, R. Böer, and R. Müller, "Combination of Finite Difference and Finite Volume Techniques in Global Reactor Analysis," *Kerntechnik*, **57**, 216-222 (1992).
7. M. Aboudy, A. Galperin, and M. Segev, "A Test of Main Stream Pin Power Reconstruction Methods," *Nucl. Sci. Eng.*, 122, 395 (1996).
8. W. S. Yang, P. J. Finck, and H. Khalil, "Reconstruction of Pin Power and Burnup Characteristics from Nodal Calculations in Hexagonal Geometry," *Nucl. Sci. Eng.*, **111**, 21 (1992).
9. H. Finnemann, R. Böer, and J. Hüsken, "Finite Difference Solution of the Flux Reconstruction Problem in Nodal Reactor Analysis," *Proc. Joint Int. Conf. on Mathematical Methods and Supercomputing in Nuclear Applications*, Karsruhe, Germany, April 19-23, 1993, Vol. 1, p. 533, Kernforschungszentrum (1993).
10. M. Yamaoka et. al., "A Method for Evaluation

of Fuel Pin-wise Power Distribution in Fast Reactors," *Proc. Intl. Conf. on the Physics of Reactors*, Mito, Japan, September 16-20, 1996, Vol. 1, p. A-278, Japan Atomic Energy Research Institute (1996).

11. R. D. Lawrence, "The DIF3D Nodal Neutronics Option for Two- and Three-Dimensional Diffusion Theory Calculations in Hexagonal Geometry," ANL-83-1, Argonne National Laboratory (March 1983).
12. K. L. Derstine, "DIF3D: A Code to Solve One-, Two-, and Three-Dimensional Finite-Difference Diffusion Theory Problems," ANL-82-64, Argonne National Laboratory (April 1984).
13. P. J. Davis, *Interpolation and Approximation*, Dover Publications, Inc., New York (1975)
14. M. Tinkham, *Group Theory and Quantum Mechanics*, McGraw-Hill Inc., New York (1964).
15. P. Lancater and K. Salkauskas, *Curve and Surface Fitting*, Academic Press, San Diego, California (1988).
16. D. C. Wade, " Overview of Advanced LMR Design in the U.S.," *Proc. Int. Reactor Physics Conf.*, Jackson Hole, Wyoming, September 18-22, 1988, Vol. I, p. 159, American Nuclear Society (1988).